Int J Coal Sci Technol (2014) 1(1):13–22
DOI 10.1007/s40789-014-0007-4

Composition and mode of occurrence of minerals in Late Permian coals from Zhenxiong County, northeastern Yunnan, China

Tian Li · Shi-Feng Dai · Jian-Hua Zou · Sen Zhang · He-Hing Tian · Li-Xin Zhao

Received: 30 October 2013 / Revised: 15 December 2013 / Accepted: 20 December 2013 / Published online: 13 September 2014

Abstract Minerals in the Late Permian coals from the Niuchang-Yigu mining area, Zhenxiong County, northeastern Yunnan, China, were investigated using optical microscopy and low temperature ashing plus X-ray diffraction (LTA + XRD). The results showed that minerals in the coal LTAs are mainly quartz, kaolinite, chamosite, mixed-layer illite/smectite (I/S), pyrite, and calcite, with trace amounts of marcasite, dolomite, and bassanite. The authigenic quartz generally occurs in collodetrinite or as a filling in cleats or cell cavities. This silica was mainly derived from aqueous solutions produced by the weathering of basaltic rocks in the Kangdian Upland and from hydrothermal fluids. The presence of β-quartz paramorph grains in collodetrinite probably indicates that these grains were detrital and came from a volcanic ash. Clay minerals are generally embedded in collodetrinite and occur as cell-fillings. Pyrite occurs as framboidal, anhedral, and euhedral grains and a cell-filling. The coals are high in pyrite and the high pyrite content probably results from seawater invading during the stage of peat accumulation. Calcite generally occurs as vein-fillings, indicating an epigenetic origin.

Keywords Late Permian coals · Minerals in coal · Zhenxiong of Yunnan

1 Introduction

Understanding the abundance and occurrence modes of minerals in coal is significant both academically for developing conjectures concerning coal-forming processes and pragmatically for optimizing coal utilization (Ren 1996; Ward 2002; Dai et al. 2012c).

T. Li (✉) · J. Zou · S. Zhang · H. Tian
Chongqing Key Laboratory of Exogenic Mineralization and Mine Environment, Chongqing Institute of Geology and Mineral Resources, Chongqing 400042, China
e-mail: lt_litian@163.com

T. Li · S. Dai · L. Zhao
State Key Laboratory of Coal Resources and Safe Mining, China University of Mining and Technology, Beijing 100083, China

T. Li · J. Zou · S. Zhang · H. Tian
Chongqing Research Center of State Key Laboratory of Coal Resources and Safe Mining, Chongqing 400042, China

There are large coal resources in southwestern China in Yunnan Province, resources second in abundance only to those in neighboring Guizhou Province (Fig. 1). The coal-bearing strata in Yunnan are Carboniferous, Permian, Triassic, and Neogene in age. The major sediment source for the Eastern Yunnan region, which was an important coal accumulation area in the Late Permian, was the Kangdian Upland (China Coal Geology Bureau 1996). Previous work on the origin and mode of occurrence of mineral matter in the Late Permian coals from eastern Yunnan includes that of Chen et al. (1992), Dai and Chou (2007), Dai et al. (2008, 2014), and Wang et al. (2012, 2013). Tonsteins derived from pyroclastics in the Late Permian coal seams from eastern Yunnan have also been studied (Zhou 1999; Zhou and Ren 1983; Zhou et al. 1982, 1990; Dai et al. 2014). In this paper, we present new data on the abundances, origin, and mode of occurrence of minerals in coal from two cores, the "NYa" and "NYb" holes drilled through the Longtan and Changxing Formations in the Niuchang-Yigu mining area, Zhenxiong County, northeastern Yunnan.

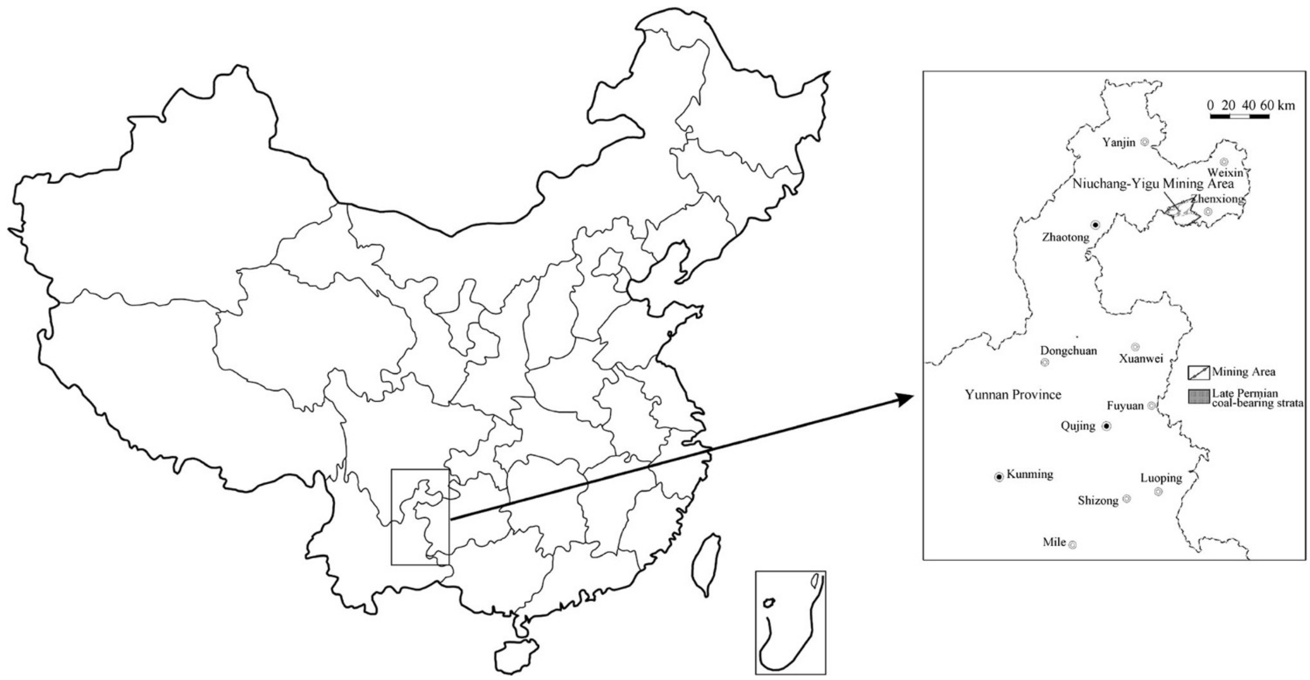

Fig. 1 Location of Niuchang-Yigu mining area, Zhenxiong County, northeastern Yunnan

2 Geological setting

The Niuchang-Yigu mining area is located in Zhenxiong County, northeastern Yunnan Province (Fig. 1). The Longtan and Changxing Formations are the major coal-bearing sequences of Late Permian age in this area (Fig. 2.; China Coal Geology Bureau 1996). The Longtan Formation mainly consists of fine-grained sandstone, siltstone, mudstone, sandy mudstone, carbonaceous mudstone and coal seams and has a thickness of > 230 m in borehole NYa and 202 m in hole NYb (Fig. 2). The Longtan Formation has a disconformable contact with the underlying Late Permian Xuanwuyan Formation and a conformable contact with the overlying Changxing Formation.

3 Sampling and analytical procedures

The coal samples were collected from two drill cores (the NYa and NYb holes) (Fig. 2). Four coal samples, NYa 2, NYa 3, NYa 4, and NYa 5, were collected from the NYa drill hole. Seven samples (NYb C3, NYb C5a, NYb C5b, NYb C6, NYb C7a, NYb C7b, and NYb C8a) were collected from NYb. The NYb C3 coal is from the Changxing Formation and the other coals are in the Longtan Formation (Fig. 2).

The proximate analyses, which determine moisture, volatile matter, and ash yield, were conducted according to Chinese Standards GB/T 212-2008 (2008). The total sulfur content was determined following Chinese Standards GB/T 214-1996 (1996). The content of C, H, and N was determined with a Vario MACRO elemental analyzer.

Polished grain mounts were prepared following Chinese Standards GB/T 474-2008 (2008) for microscopic analysis. Mean random reflectance of vitrinite was determined using a Craic QDI 302™ spectrophotometer attached to a Leica DM-4500P microscope at a magnification of 500×. The standard reference gadolinium gallium garnet (manufactured by Klein & Becker) with a calculated standard reflectance of 1.722 % at $\lambda = 546$ nm in oil immersion was used for calibrating the vitrinite reflectance spectra.

Maceral components were identified using white-light reflectance microscopy in oil. The maceral classification and terminology are based on Taylor et al. (1998) and the ICCP System 1994 (International Committee for Coal and Organic Petrology (ICCP 1998, 2001).

Mineralogy was determined by optical microscopy and X-ray powder diffraction (XRD). Low-temperature ashing (LTA) of coal was performed using an EMITECH K1050X plasma asher prior to XRD analysis. XRD analysis was performed with a Rigaku D/max 2500pc powder diffractometer using Ni-filtered Cu-Kα radiation and a scintillation detector. The XRD pattern was recorded in a 2θ range of 2.6–70°, with a step size of 0.01°. X-ray diffractograms of the LTAs were subjected to quantitative mineralogical analysis using Siroquant™ commercial interpretation software developed by Taylor (1991) based on the principles for diffractogram profiling set out by Rietveld (1969).

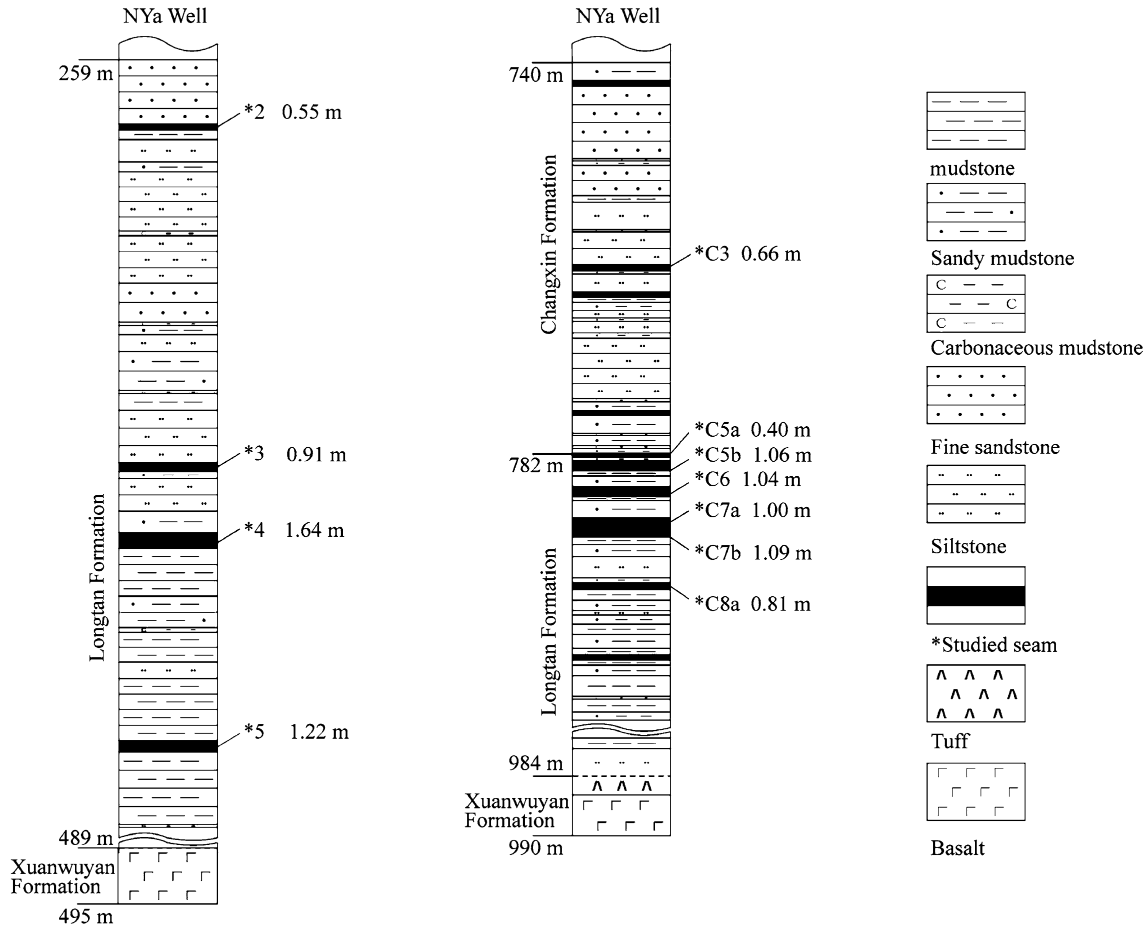

Fig. 2 Sedimentary sequences in the Niuchang-Yigu mining area

Further details describing the use of this technique for coal-related materials are given by Ward et al. (1999, 2001) and Ruan and Ward (2002).

4 Results and discussion

4.1 Coal chemistry

Proximate and ultimate analyses results, total sulfur, the gross calorific values, and random vitrinite reflectance data for the Niuchang-Yigu coals are shown in Table 1.

The weighted averages of moisture, volatile matter, gross calorific value, and random vitrinite reflectance are 0.86 %, 12.06 %, 22.46 MJ/kg, and 2.25 %, respectively. The ash yield from Niuchang-Yigu coals is high, ranging from 23.53 % to 48.63 %, with a weighted average of 34.92 %. The total sulfur content of the coals ranges from 0.07 % to 6.27 %, with an average of 2.45 %. According to Chinese Standard GB/T 15224.1-2010 (2010), the NYa 4, NYb C7a, and NYb C7b samples are medium-ash coals (20.01 % $< A_d \leq$ 30.00 %), whereas the NYa 2 and NYa 5 samples are high-ash coals (40.01 % $< A_d \leq$ 50.00 %). The other samples are medium–high ash coals (30.01 % $< A_d \leq$ 40.00 %). According to Chinese Standard GB/T 15224.2-2010 (2010), the special-low-, low-, medium-, medium–high-, and high-sulfur coals have $\leq$ 0.50 %, 0.51 %–1.00 %, 1.01 %–2.00 %, 2.01 %–3.00 %, and $>$ 3.00 % total sulfur contents, respectively. According to this standard, more than half of the samples analyzed are medium–high- and high-sulfur coals.

4.2 Maceral composition

Maceral compositions are presented in Table 2. The weighted average of the vitrinite and inertinite contents in Niuchang-Yigu coals are 71.3 and 28.7 %, respectively.

The vitrinite is dominated by collodetrinite (Fig. 3a), collotelinite (Fig. 3a), and vitrodetrinite, with traces of telinite and corpogelinite (Fig. 3b). Corpogelinite was observed in only two samples, NYb C3 and NYb C5a; the abundances in those samples being 1.1 % and 0.4 %, respectively. The inertinite is mainly composed of fusinite (Fig. 3a), inertodetrinite (Fig. 3a), and semifusinite (Fig. 3d), along with a trace amount of macrinite (Fig. 3c).

Table 1 Proximate and ultimate analyses (%), total sulfur (%), gross calorific values (MJ/kg), and random vitrinite reflectance (%) in the Niuchang-Yigu coals

Samples	Thickness (m)	M_{ad}	A_d	V_{daf}	C_{daf}	H_{daf}	N_{daf}	$S_{t,d}$	$Q_{gr,d}$	$R_{o,ran}$
NYa 2	0.55	0.76	48.63	13.71	87.71	3.93	1.55	2.53	17.57	2.19
NYa 3	0.91	0.89	30.95	11.01	88.00	3.49	1.39	3.14	24.23	2.34
NYa 4	1.64	1.01	25.76	10.67	90.25	3.61	1.61	0.54	26.19	2.48
NYa 5	1.22	0.84	47.91	14.77	86.20	4.83	1.35	0.07	17.60	2.23
NYb C3	0.66	0.84	38.45	13.02	86.81	4.15	1.69	3.62	21.24	2.34
NYb C5a	0.40	0.77	39.37	10.45	88.39	3.69	1.54	1.58	20.58	2.48
NYb C5b	1.06	0.93	34.99	15.38	83.64	3.71	1.32	6.27	21.89	2.23
NYb C6	1.04	0.75	31.14	11.03	85.68	3.61	1.29	4.94	23.35	2.35
NYb C7a	1.00	0.84	28.92	10.14	87.30	3.71	1.43	2.45	24.55	2.39
NYb C7b	1.09	1.01	23.53	11.41	89.22	4.19	2.23	1.15	26.60	2.39
NYb C8a	0.81	0.77	34.49	11.09	90.35	3.55	1.73	0.63	23.23	2.46
WA		0.86	34.92	12.06	87.60	3.86	1.56	2.45	22.46	2.35

M moisture, *A* ash yield, *V* volatile matter, *C* carbon, *H* hydrogen, *N* nitrogen, S_t total sulfur, *ad* air-dry basis, *d* dry basis, *daf* dry and ash-free basis, $Q_{gr,d}$ gross calorific value, on dry basis, $R_{o,ran}$ random reflectance of vitrinite, *WA* weighted average

Table 2 Maceral compositions in the Niuchang-Yigu coals (vol. %, on mineral-free basis)

Samples	Cd	Ct	Cg	T	Vd	V	F	Sf	Mac	Id	I
NYa 2	43.5	2.5	bdl	1.9	18.0	65.8	12.4	9.3	1.9	10.6	34.2
NYa 3	54.6	9.2	bdl	5.6	5.1	74.5	11.2	3.1	2.0	9.2	25.5
NYa 4	45.1	14.5	bdl	6.7	3.3	69.6	11.4	10.3	1.7	7.0	30.4
NYa 5	49.1	1.8	bdl	0.9	13.4	65.2	17.0	3.6	0.9	13.4	34.8
NYb C3	55.3	10.6	1.1	1.8	4.4	73.3	11.4	4.4	4.8	6.2	26.7
NYb C5a	45.9	10.1	0.4	1.1	3.0	60.4	28.4	3.7	3.7	3.7	39.6
NYb C5b	62.3	6.2	bdl	bdl	6.8	75.3	16.7	3.1	0.6	4.3	24.7
NYb C6	69.3	5.1	bdl	bdl	bdl	74.5	17.5	0.7	0.7	6.6	25.5
NYb C7a	54.5	10.1	bdl	2.2	3.9	70.8	20.8	3.9	1.7	2.8	29.2
NYb C7b	50.6	19.7	bdl	2.5	2.5	75.3	10.9	5.4	2.9	5.4	24.7
NYb C8a	65.6	5.4	bdl	bdl	9.1	80.1	8.6	0.5	2.2	8.6	19.9
WA	54.2	8.7	0.3	2.1	6.3	71.3	15.1	4.4	2.1	7.1	28.7

Cd collodetrinite, *Ct* collotelinite, *Cg* corpogelinite, *T* telinite, *Vd* vitrodetrinite, *V* total vitrinite, *F* fusinite, *Sf* semifusinite, *Mac* macrinite, *Id* inertodetrinite, *I* total inertinite, *WA* weighted average, *bdl* below detection limit

4.3 Minerals in low temperature ash of Niuchang-Yigu coal

The minerals in LTAs of Niuchang-Yigu coal are mainly quartz, kaolinite, chamosite, mixed-layer illite/smectite (I/S), pyrite and calcite, with trace amounts of marcasite, dolomite and bassanite (Table 3).

4.3.1 Quartz

Quartz is a common mineral in most coals (Ren 1996; Tang and Huang 2004). In general, quartz is mainly of terrigenous detrital origin (Ren 1996) but authigenic quartz is quite common in the Late Permian coals from eastern Yunnan (Ren 1996; Dai and Chou 2007; Dai et al. 2008, 2014).

The quartz content of LTAs of Niuchang-Yigu coals is between 33.2 % and 67.6 %, with a weighted average of 48.8 %, an average close to that of the Late Permian coals from the Taoshuping area (43.8 %; Wang et al. 2012). Quartz in the Niuchang-Yigu coals has three main modes of occurrence, (1) embedded in collodetrinite with a variety of shapes (Fig. 4a), (2) as cell- and cleat-fillings (Fig. 4b, d), and (3) coexisting with pyrite and clay minerals (Fig. 4f). These modes of occurrence suggest an authigenic origin. The authigenic quartz in eastern Yunnan coals was derived from silica-containing solutions produced by the weathering of basaltic rocks in the Kangdian Upland (Ren

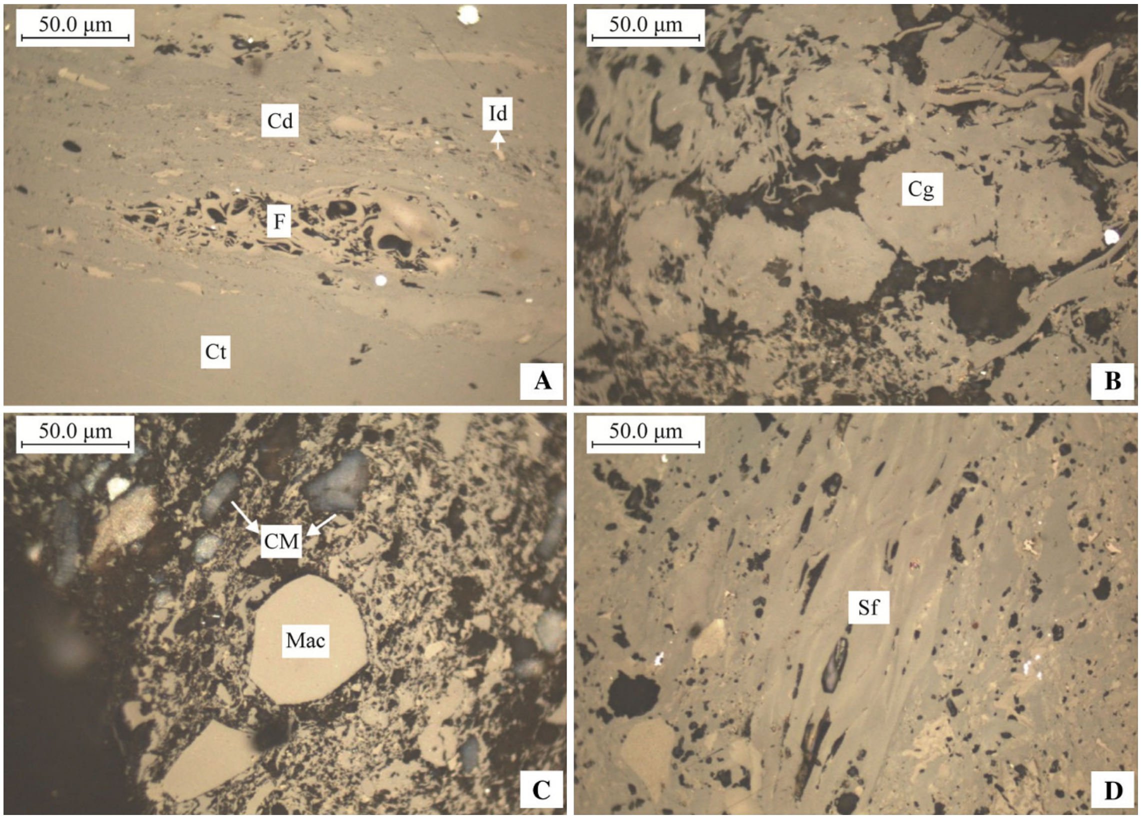

Fig. 3 Photomicrographs of macerals in the Niuchang-Yigu coals. **a** *Cd* collodetrinite, *Ct* collotelinite, *F* fusinite, and *Id* inertodetrinite in sample NYb C7b coal; reflected light, oil immersion. **b** *Cg* corpogelinite in sample NYb C3 coal; reflected light, oil immersion. **c** *Mac* macrinite and detrital *CM* carbonate minerals in sample NYb C7b coal; reflected light, oil immersion. **d** *Sf* semifusinite in sample NYb C3 coal; reflected light, oil immersion

Table 3 Low temperature ash yield (%) and mineral compositions of LTAs of Niuchang-Yigu coal by XRD analysis (%; on organic matter-free basis)

Samples	LTA yield	Quartz	Kaolinite	Chamosite	I/S	Pyrite	Calcite	Marcasite	Dolomite	Bassanite
NYa 2	52.18	67.6	bdl	4.4	16.5	7.7	3.6	bdl	0.2	bdl
NYa 3	33.79	60.8	12.5	2.8	6.9	11.1	1.2	4.7	bdl	bdl
NYa 4	28.10	37.2	29.8	7.4	19.4	2.1	4.2	bdl	bdl	bdl
NYa 5	50.81	38.0	38.7	9.0	14.0	bdl	0.3	bdl	bdl	bdl
NYb C3	42.10	58.5	bdl	7.9	11.6	15.5	3.4	1.5	bdl	1.6
NYb C5a	43.19	57.8	7.7	7.3	bdl	7.2	14.3	bdl	5.7	bdl
NYb C5b	42.40	33.2	10.9	3.1	16.6	25.5	3.6	bdl	0.8	6.2
NYb C6	37.78	49.3	7.1	1.8	bdl	17.5	14.6	3.8	0.9	5.1
NYb C7a	33.23	40.4	22.6	9.0	bdl	7.4	10.5	3.8	0.5	5.8
NYb C7b	26.26	35.5	44.7	8.8	bdl	3.9	5.9	bdl	0.3	1.0
NYb C8a	36.23	58.8	25.5	10.4	bdl	2.0	3.3	bdl	bdl	bdl
WA	38.73	48.8	18.2	6.5	7.8	9.1	5.9	1.3	0.8	1.8

WA weighted average, *bdl* below detection limit

1996) and then precipitated from hydrothermal fluids (Dai and Chou 2007; Dai et al. 2008). Most of the detrital quartz found in the coals also originated from the weathering of basaltic rocks in the Kangdian Upland (Fig. 4c).

Some quartz grains distributed in the collodetrinite have a well-developed β-quartz crystal paramorph. This crystal form probably indicates a volcanic origin for these grains (Fig. 4c). Several tonstein layers deposited in the middle-

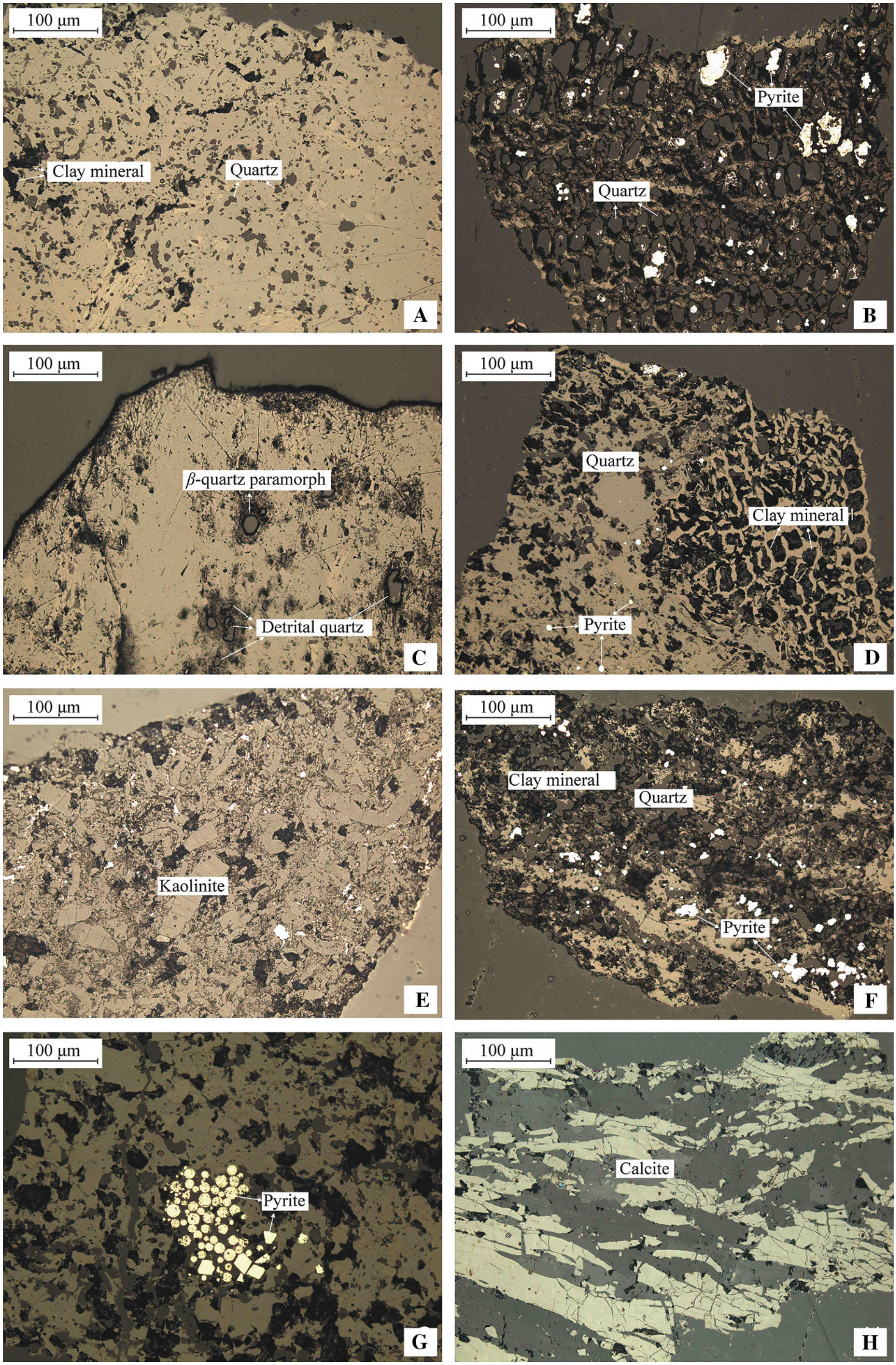
100 μm
Clay mineral
Quartz
A
100 μm
Pyrite
Quartz
B
100 μm
β-quartz paramorph
Detrital quartz
C
100 μm
Quartz
Clay mineral
Pyrite
D
100 μm
Kaolinite
E
100 μm
Clay mineral
Quartz
Pyrite
F
100 μm
Pyrite
G
100 μm
Calcite
H

◀**Fig. 4** Photomicrographs of minerals in the Niuchang-Yigu coals. **a** quartz grains with different shapes and clay minerals embedded in collodetrinite in sample NYb C7b coal; reflected light. **b** quartz and pyrite as cell-fillings in sample NYa 3 coal; reflected light. **c** Well-developed crystal of β-quartz and detrital quartz in collodetrinite in sample NYa 5 coal; reflected light. **d** cleat-filling quartz, cell-filling clay minerals, and isolated framboidal pyrite in sample NYb C5a coal; reflected light. **e** Vermicular kaolinite in sample NYb C7b coal; reflected light. **f** quartz along with pyrite and clay minerals in sample NYa 3 coal; reflected light. **g** irregular massive lumps of clay minerals and framboidal and euhedral pyrite in collodetrinite in sample NYb C5a coal; reflected light. **h** calcite occurs as vein-fillings in sample NYb C5a coal; plane-polarized and reflected light

late to Late Permian coal seams in this area (Zhou et al. 2000; Dai et al. 2014), demonstrate that there had been frequent volcanic eruptions during the Late Permian.

4.3.2 Clay minerals

Clay minerals in the LTAs of Niuchang-Yigu coal include kaolinite, mixed-layer I/S, and chamosite. The clay mineral content ranges from 8.9 % to 61.7 %, with a weighted average of 32.5 % (Table 3). In the coals studied, the clays occur in three different modes. They occur as irregular massive lumps in collodetrinite (Fig. 4a), as cell-fillings (Fig. 4d), and as clots coexisting with quartz and pyrite (Fig. 4f). Vermicular kaolinite was also found in the coal (Fig. 4e).

Kaolinite is the dominant clay mineral in most Niuchang-Yigu samples except for samples NYa 2 and NYb C3. The kaolinite content ranges from below detection limit (bdl) to 38.7 % and from bdl to 44.7 % in the LTAs of NYa and NYb cores, respectively. In general, the kaolinite content is roughly vertically zoned increasing from top to bottom in both holes.

Chlorite, with the two common forms being chamosite and clinochlore, is generally uncommon in coal (Bouška et al. 2000; Tang and Huang 2004) but it is present in our samples. Chamosite has the same diffraction peaks as clinochlore in XRD patterns but it can be identified by its weaker odd-order peaks (the 001 and 003 peaks) and stronger even-order peaks (the 002 and 004 peaks) in X-ray diffractograms (Dai and Chou 2007; Moore and Reynolds 1989). Figure 5 shows that the chlorite in this study is chamosite, which is actually common in the Late Permian coals from eastern Yunnan (Dai and Chou 2007; Dai et al. 2008, 2014; Wang et al. 2012, 2013).

Chamosite exists in each coal seam examined for this study with the content ranging from 1.8 % to 10.4 % (average of 6.5 %) and reaching its highest values in the lower coals in the both holes (sample NYa 5 at 9.0 % and NYb C8a at 10.4 %). The mode of occurrence of the chamosite, coexisting with kaolinite as cell-fillings, indicates that it is the product of Fe- and Mg-rich solutions that probably originated from volcanic activity (Dai and Chou 2007; Dai et al. 2008).

The mixed-layer I/S is an intermediate product in the smectite to illite transformation process. It is commonly observed in the coal LTAs of the NYa hole, and its content ranges from 6.9 % to 19.4 %. However, it appears only in two samples in hole NYb, (NYb C3 and NYb C5b). Mixed-layer I/S is also common in other Late Permian coals from eastern Yunnan (Dai and Chou 2007; Dai et al. 2008; Wang et al. 2012), and is the dominant clay mineral in Changxing coal (Wang et al. 2013). There it generally occurs as thin beds, massive lenses, and fracture- or cell-fillings (Wang 2011).

4.3.3 Pyrite, marcasite and bassanite

The content of pyrite in the LTAs ranges from bdl to 25.5 % (mean 9.1 %), lower than that of quartz and kaolinite (Table 3). It is, however, relatively high in the LTAs

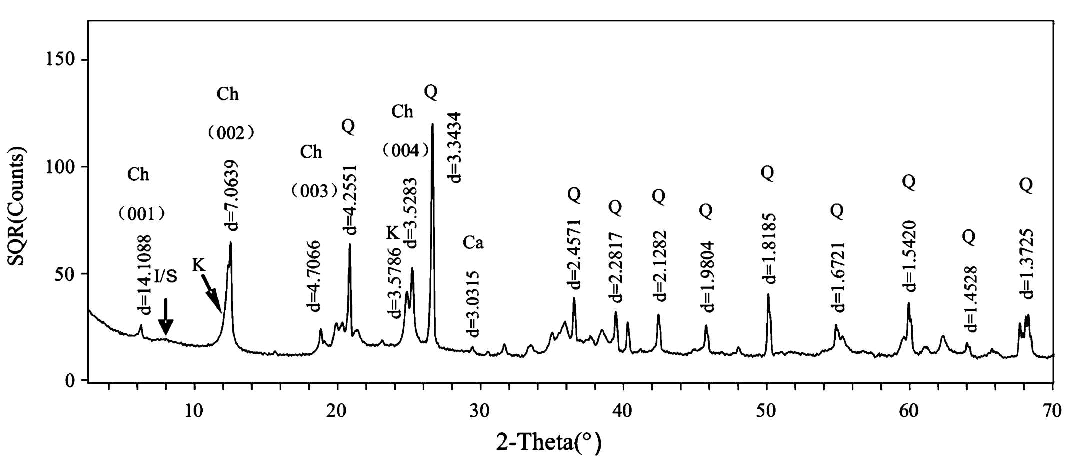

Fig. 5 XRD pattern of LTA of sample NYa 5 coal. *Ch* chamosite, *I/S* illite-smectite, *K* kaolinite, *Q* quartz, *Ca* calcite

of high-sulfur coals including the NYa 3, NYb C3, NYb C5a, and NYb C6 samples (11.1 %, 15.5 %, 25.5 %, and 17.5 %, respectively). The pyrite-total sulfur correlation coefficient (r) is 0.99—essentially all of the sulfur in the coal is contained in pyrite.

In our samples pyrite occurs in framboidal, anhedral and euhedral forms (Fig. 4d, f, g), and also as cell-fillings (Fig. 4b). Dai and Chou (2007) also found pyritized algae in the coals from this area. The high pyrite content is probably due to the invasion of seawater during early diagenesis (Dai and Chou 2007; Ren 1996).

Although having the same chemical compositions, marcasite and pyrite can be differentiated by both optical microscopy and XRD (Ward 2002; Fig. 6). Marcasite is present in at least four LTAs (NYa 3, NYb C3, NYb C6, and NYb C7a identified by XRD analysis), with the content in those four samples being 4.7 %, 1.5 %, 3.8 %, and 3.8 %, respectively. Marcasite commonly exists in the coal LTAs which have high content of pyrite as well. However, sample NYb C5b has the highest pyrite content, but the marcasite content is below detection limit in that sample.

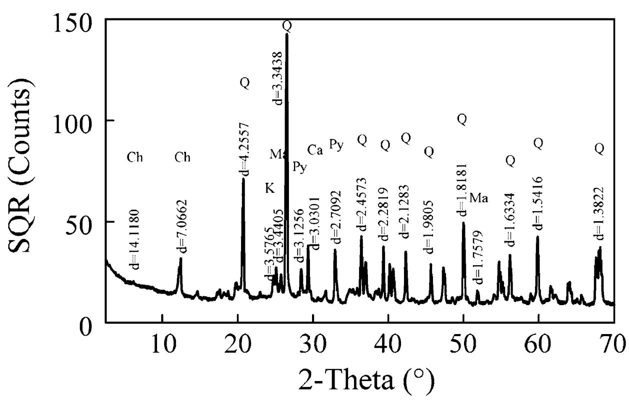

Fig. 6 XRD pattern of LTA of the sample NYa 3 coal. *Ch* chamosite, *K* kaolinite, *Q* quartz, *Ma* marcasite, *Py* pyrite, *Ca* calcite

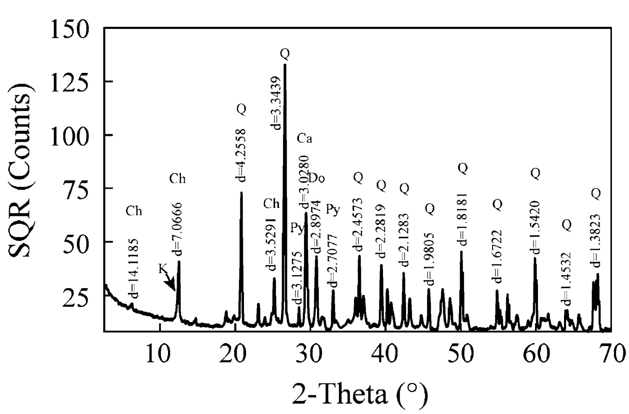

Fig. 7 XRD pattern of LTA of the sample NYb C5a coal. *Ch* chamosite, *K* kaolinite, *Q* quartz, *Py* pyrite, *Ca* calcite, *Do* dolomite

The content of bassanite in the LTAs is from bdl to 6.2 % (mean 1.3 %; Table 3). It has also been identified in LTAs of some other Chinese coal such as the Wulantuga and Guanbanwusu coals in Inner Mongolia and the Fusui coals in Guangxi (Dai et al. 2012a, 2012b, 2013). It is commonly thought that the bassanite in the coal LTAs was formed in the plasma-ashing process (Ward et al. 2001; Ward 2002).

4.3.4 *Calcite and dolomite*

The carbonate minerals in the LTAs are calcite and dolomite, with a weighted average content of 5.6 % and 0.8 %, respectively (Table 3). The calcite content ranges from 3.3 % to 14.6 % in the LTAs of NYb core, much higher than that in the NYa core (0.3 %–4.2 %). Although the dolomite content in most of the LTAs is low, sample NYb C5a has a high content of 5.7 % (Fig. 7, Table 3). The calcite mainly occurs as vein-fillings, (Fig. 4h), indicating an epigenetic origin. Detrital calcite is only rarely observed in coal as it can be easily decomposed in the acid environment of a peat mire (Kortenski 1992; Bouška et al. 2000). However, detrital carbonate grains do occur in some of our samples in the collodetrinite (Fig. 3c) and are present in other Late Permian coals from eastern Yunnan (Wang 2011).

5 Conclusions

Most coals analyzed for this study have high total sulfur contents and high ash yields. Vitrinite is the dominant maceral group in all the coals, followed by inertinite. The minerals in LTAs of Niuchang-Yigu coals are mainly quartz, kaolinite, chamosite, mixed-layer I/S, pyrite, and calcite, with trace amounts of marcasite, dolomite, and bassanite. Quartz is mainly embedded in collodetrinite and occurs as cleat- and cell-fillings. The silica was primarily transported by aqueous solutions originated from the weathering of basaltic rocks in the Kangdian Upland and by hydrothermal fluids. The presence of β-quartz paramorph grains, distributed in collodetrinite, probably indicates that quartz from volcanic ash was deposited during peat accumulation. Clay minerals generally occur in collodetrinite and as fill in coal-forming plant cells. The chamosite was the product of Fe- and Mg-rich solutions that were probably generated by volcanic activity. In most cases, pyrite occurs as framboidal, anhedral, and euhedral particles in collodetrinite but it also is present as cell-fillings. The high pyrite content is probably the result of seawater invasion during early diagenesis. A small proportion of the carbonate minerals present occur as detrital grains in collodetrinite but most of the calcite occurs as vein-fillings and no doubt has an epigenetic hydrothermal origin.

Acknowledgments This research was supported by the National Key Basic Research and Development Program (No. 2014CB238902), National Natural Science Foundation of China (Nos. 41272182 and 40930420), and the Program for Changjiang Scholars and Innovative Research Team in University.

References

Bouška V, Pešek J, Sykorova I (2000) Probable modes of occurrence of chemical elements in coal. Acta Mont. Serie B Fuel Carbon Miner Process Praha 10:53–90

Chen SQ, Chen JH, Zhao SJ (1992) Occurrence character of pyrite in coal of the upper part of the Late Permian coal measures in eastern Ynnan and western Guizhou. Bull Yichang Inst Geol Miner Resour (CAGS) 18:135–145 (in both Chinese and English)

China Coal Geology Bureau (1996) Sedimentary environments and coal accumulation of Late Permian coal formation in Western Guizhou, Southern Sichuan and Eastern Yunnan, China. Chongqing University Press, Chongqing (in Chinese with English abstract)

Chinese Standard GB/T 15224.1-2010 (2010) Classification for quality of coal. Part 1: Ash (in Chinese)

Chinese Standard GB/T 15224.2-2010 (2010) Classification for quality of coal. Part 2: Sulfur content (in Chinese)

Chinese Standard GB/T 212-2008 (2008) Proximate analysis of coal (in Chinese)

Chinese Standards GB/T 214-1996 (1996) Determination of total sulfur in coal (in Chinese)

Chinese Standards GB/T 474-2008 (2008) Method for preparation of coal sample (in Chinese)

Dai SF, Chou CL (2007) Occurrence and origin of minerals in a chamosite-bearing coal of Late Permian age, Zhaotong, Yunnan, China. Am Miner 92:1253–1261

Dai SF, Tian LW, Chou CL, Zhou YP, Zhang MQ, Zhao L, Wang JM, Yang Z, Cao HZ, Ren DY (2008) Mineralogical and compositional characteristics of Late Permian coals from an area of high lung cancer rate in Xuan Wei, Yunnan, China: occurrence and origin of quartz and chamosite. Int J Coal Geol 76:318–327

Dai SF, Wang XB, Seredin VV, Hower JC, Ward CR, O'keefe MKJ, Huang WH, Li T, Li X, Liu HD, Xue WF, Zhao LX (2012a) Petrology, mineralogy, and geochemistry of the Ge-rich coal from the Wulantuga Ge ore deposit, Inner Mongolia, China: new data and genetic implications. Int J Coal Geol 90–91:72–99

Dai SF, Jiang YF, Ward CR, Gu LD, Seredin VV, Liu HD, Zhou D, Wang XB, Sun YZ, Zou JH, Ren DY (2012b) Mineralogical and geochemical compositions of the coal in the Guanbanwusu Mine, Inner Mongolia, China: further evidence for the existence of an Al (Ga and REE) ore deposit in the Jungar coalfield. Int J Coal Geol 98:10–40

Dai SF, Ren DY, Chou CL, Finkelman RB, Seredin VV, Zhou YP (2012c) Geochemistry of trace elements in Chinese coals: a review of abundances, genetic types, impacts on human health, and industrial utilization. Int J Coal Geol 94:3–21

Dai SF, Zhang WG, Ward CR, Seredin VV, Hower JC, Li X, Song WJ, Wang XB, Kang H, Zheng LC, Wang PP, Zhou D (2013) Mineralogical and geochemical anomalies of late Permian coals from the Fusui Coalfield, Guangxi Province, southern China: influences of terrigenous materials and hydrothermal fluids. Int J Coal Geol 105:60–84

Dai SF, Li T, Seredin VV, Ward CR, Hower JC, Zhou YP, Zhang MQ, Song XL, Song WJ, Zhao CL (2014) Origin of minerals and elements in the Late Permian coals, tonsteins, and host rocks of the Xinde Mine, Xuanwei, eastern Yunnan, China. Int J Coal Geol 121:53–78

International Committee for Coal and Organic Petrology (ICCP) (1998) The new vitrinite classification (ICCP System 1994). Fuel 77:349–358

International Committee for Coal and Organic Petrology (ICCP) (2001) The new inertinite classification (ICCP System 1994). Fuel 80:459–471

Kortenski J (1992) Carbonate minerals in Bulgarian coals with different degrees of coalification. Int J Coal Geol 20:225–242

Moore DM, Reynolds RC (1989) X-ray diffraction and the identification and analysis of clay minerals. Oxford University Press, New York

Ren DY (1996) Mineral matters in coal. In: Han DX (ed) Coal Petrology of China. Publishing House of China University of Mining and Technology, Xuzhou, pp 67–77 (in Chinese with English abstract)

Rietveld HM (1969) A profile refinement method for nuclear and magnetic structures. J Appl Crystallogr 2:65–71

Ruan CD, Ward CR (2002) Quantitative X-ray powder diffraction analysis of clay minerals in Australian coals using Rietveld methods. Appl Clay Sci 21:227–240

Tang XY, Huang WH (2004) Trace elements in Chinese coals. The Commercial Press, Beijing (in Chinese)

Taylor JC (1991) Computer programs for standardless quantitative analysis of minerals using the full powder diffraction profile. Powder Diffr 6:2–9

Taylor GH, Teichmüller M, Davis A, Diessel CFK, Littke R, Robert P (1998) Organic Petrology. Gebrüder Borntraeger, Berlin 704

Wang XB (2011) Enrichment and differentiation mechanism of mineral matter in the Late Permian coals from Eastern Yunnan Province. Doctor's Thesis, China University of Mining and Technology, Beijing (in Chinese with English abstract)

Wang XB, Dai SF, Chou CL, Zhang MQ, Wang JM, Song XL, Wang W, Jiang YF, Zhou YP, Ren DY (2012) Mineralogy and geochemistry of Late Permian coals from the Taoshuping Mine, Yunnan Province, China: evidences for the sources of minerals. Int J Coal Geol 96–97:49–59

Wang XB, Zhang MQ, Zhang WG, Wang JM, Zhou YP, Song XL, Li T, Li X, Liu HD, Zhao LX (2013) Occurrence and origins of minerals in mixed-layer illite/smectite-rich coals of the Late Permian age from the Changxing Mine, eastern Yunnan, China. Int J Coal Geol 102:26–34

Ward CR (2002) Analysis and significance of mineral matter in coal seams. Int J Coal Geol 50:135–168

Ward CR, Spears DA, Booth CA, Staton I, Gurba LW (1999) Mineral matter and trace elements in coals of the Gunnedah Basin, New South Wales, Australia. Int J Coal Geol 40:281–308

Ward CR, Taylor JC, Matulis CE, Dale LS (2001) Quantification of mineral matter in the Argonne Premium coals using interactive Rietveld-based X-ray diffraction. Int J Coal Geol 46:67–82

Zhou YP (1999) The synsedimentary alkalinity-volcanic ash derived tonsteins of early Longtan age in South-western China. Coal geol Explor 27:5–9 (in Chinese with English abstract)

Zhou YP, Ren YL (1983) Genesis and distribution of tonsteins in late-Permian coalfields in Southwestern China. J China Coal Soc 8:76–88 (in Chinese with English abstract)

Zhou YP, Ren YL, Bohor BF (1982) Origin and distribution of tonsteins in Late Permian coal seams of Southwestern China. Int J Coal Geol 2:49–77

Zhou YP, Tang DZ, Burger K (1990) Synsedimentary volcanic ash-derived illite tonsteins in late Permian coal-bearing deposits of southwestern China. Acta Sedimentol Sin 8:85–93 (in Chinese with English abstract)

Zhou YP, Bohor BF, Ren YL (2000) Trace element geochemistry of altered volcanic ash layers (tonsteins) in Late Permian coal-bearing formations of eastern Yunnan and western Guizhou Province, China. Int J Coal Geol 44:305–324